Initiation of Minus-Strand DNA Synthesis by Human Immunodeficiency Virus Type 1 Reverse Transcriptase†

Joseph A. Vaccaro, Hansi A. Singh, and Karen S. Anderson*

Department of Pharmacology, Yale University School of Medicine, 333 Cedar Street, New Haven, Connecticut 06520-8066

Received April 26, 1999; Revised Manuscript Received September 24, 1999

ABSTRACT: The initiation of (−) strand DNA synthesis by HIV-1 reverse transcriptase was examined using a transient kinetic approach and a physiologically relevant RNA 18-mer/RNA 36-mer primer-template substrate. HIV-1 reverse transcriptase (RT) was found to bind with reasonably high affinity to the RNA/RNA substrate (K_d = 90 nM), although the affinity for DNA/RNA and DNA/DNA substrates is higher ($K_d \approx 5$ nM). A pre-steady-state burst of deoxynucleotide incorporation ($k_{obsd} = 1.0\ s^{-1}$) into the RNA duplex was observed followed by a slower steady-state release of the elongated primer-template product ($k_{ss} = 0.58\ s^{-1}$). The observation of a burst provides evidence that the release of the product is most likely the rate-limiting step in the overall kinetic pathway for the enzymatic reaction during a single deoxynucleotide incorporation event. Furthermore, the release of this product was 5-fold faster than that for elongated DNA/RNA and DNA/DNA products. Single-turnover experiments showed that there is a hyperbolic dependence of the rate of deoxynucleotide incorporation on the concentration of dCTP and demonstrated that the maximum rate of dCTP incorporation ($k_{pol} = 1.4\ s^{-1}$) is 33- and 12-fold slower than the values for DNA/RNA and DNA/DNA primer-template substrates, respectively, while the affinity of dCTP (K_d = 780 μM) for the HIV-1 RT·RNA/RNA complex is 56- and 71-fold weaker than the affinities for HIV-1 RT·DNA/RNA and HIV-1 RT·DNA/DNA complexes, respectively. Consequently, the overall efficiency of dCTP incorporation (k_{pol}/K_d) into the RNA/RNA substrate is approximately 1800- and 800-fold less than that for DNA/RNA and DNA/DNA substrates, respectively. These findings provide evidence which suggests that the HIV-1 RT·RNA/RNA·dCTP ternary complex exists in a significantly different conformation compared to ternary complexes involving DNA/RNA and DNA/DNA substrates. A model summarizing these results is presented, and implications for the molecular mechanism of initiation of (−) strand DNA synthesis by RT are discussed.

Virally encoded human immunodeficiency virus (HIV)[1] reverse transcriptase (RT) catalyzes the conversion of the single-stranded viral RNA genome to a double-stranded DNA copy that is subsequently integrated into the host cell DNA. To ultimately form the double-stranded DNA copy, RT must catalyze both RNA-dependent and DNA-dependent DNA polymerization as well as RNase H cleavage activity to remove the RNA template once the DNA has been synthesized. Because RT is an enzyme with unique catalytic properties, it has been the target of several antiviral therapeutic agents used in the treatment of AIDS (*1*, *2*, *3*). Nucleoside analogues such as AZT (3′-azido 3′-deoxythymidine) have been the drugs of choice to inhibit viral replication. However, their long-term use is limited by toxicity (*4*, *5*) and the high frequency of viral mutation whereby drug-resistant forms of RT may accumulate (*6*). A detailed understanding of the catalytic mechanism of RT may facilitate the development of more effective antiviral drugs.

The formation of the double-stranded DNA copy of the viral RNA genome involves four distinct stages of DNA polymerization that differ from each other with respect to the specific nature of the primer-template substrate (Figure 1). HIV-1 RT initiates (−) strand DNA synthesis from an RNA/RNA primer-template duplex in which the human $tRNA^{Lys}$ serves as a primer on the RNA genome, resulting in the formation of (−) strand strong-stop DNA (stage 1). Continued synthesis of (−) strand DNA involves a DNA/RNA primer-template substrate (stage 2). Following (−) strand DNA synthesis, RT initiates (+) strand DNA synthesis from a genomic RNA primer annealed to the (−) DNA strand (stage 3). Finally, to complete both (−) and (+) strand DNA synthesis, RT utilizes a DNA/DNA primer-template substrate (stage 4).

Much insight into how an enzyme works can be gained by examining the reaction kinetics for an enzyme. A traditional steady-state kinetic analysis, however, is limited by the fact that it reflects the rate-limiting step in the overall reaction pathway. On the other hand, a transient kinetic analysis allows one to examine each of the individual steps in the reaction pathway for an enzyme including the

† This work was supported by NIH Grant GM49551 to K. S. A. and ACS Postdoctoral Fellowship PF-4478 to J. A. V.

* To whom correspondence should be addressed, 333 Cedar St., New Haven, CT 06520-8066. Telephone: 203-785-4526. Fax: 203-785-7670. E-mail: karen.anderson@yale.edu.

[1] Abbreviations: AIDS, acquired immunodeficiency syndrome; ATP, adenosine 5′-triphosphate; dCMP, 2′-deoxycytidine-5′-monophosphate; dCTP, 2′-deoxycytidine-5′-triphosphate; dNTP, 2′-deoxynucleoside-5′-triphosphate; EDTA, (ethylenediamine) tetraacetate; HIV-1, human immunodeficiency virus type 1; PBS, primer binding site; RT, reverse transcriptase; Tris, tris(hydroxymethyl)aminomethane.

10.1021/bi990945x CCC: $18.00 © 1999 American Chemical Society
Published on Web 11/09/1999

identification of enzyme intermediates and conformational changes that might be associated with chemical catalysis (*7*, *8*, *9*, *10*). Our laboratory (*11*, *12*, *13*) and others (*14*, *15*, *16*) have used a transient kinetic approach to examine the mechanism of DNA polymerization by RT using DNA/RNA (stage 2) and DNA/DNA (stage 4) primer-template substrates. These studies have shown that the reaction pathway is ordered. The first step involves the binding of the primer-template (P_n/T) substrate to the enzyme to form a tight E·P_n/T complex with a K_d value in the nanomolar range. Together, the enzyme and primer-template form a pocket at the active site that provides the necessary contacts for the binding of the correct deoxynucleoside triphosphate (*17*). The enzyme checks for proper base-pairing geometry and then undergoes a rate-determining conformational change that limits chemical catalysis. During a single deoxynucleotide incorporation event, the slowest step in the pathway involves the dissociation of the elongated primer-template substrate (P_{n+1}/T) from the enzyme and is the step which is being examined in a steady-state kinetic analysis (*18*). In the presence of all four deoxynucleoside triphosphates, the enzyme can processively extend the primer with multiple deoxynucleotides before releasing an elongated product. Earlier work has shown that the kinetic pathway for single deoxynucleotide incorporation is representative of multiple deoxynucleotide incorporations during processive DNA synthesis (*11*).

Although much has been learned of the mechanism of RT using DNA/DNA and DNA/RNA primer-template substrates, relatively little is known about the use of an RNA/RNA substrate to initiate (−) strand DNA synthesis (Figure 1, stage 1) (*19*). A kinetic study with a bovine modified $tRNA^{Lys}$ primer using subsaturating concentrations of dNTP suggested that dNTP incorporation is relatively slow compared to the incorporation of a dNTP into a short DNA primer (*20*). It was unclear, however, whether this slow rate was the result of attaching a dNTP to RNA or the presence of the bulky tRNA primer and a long RNA template (>300 nucleotides). More recently, an elegant and comprehensive pre-steady-state kinetic study was conducted using a series of RNA/RNA, DNA/RNA, and DNA/DNA primer-template substrates (*21*). It was shown that the rate of dNTP incorporation using an RNA/RNA duplex substrate is relatively slow and the affinity of the incoming dNTP is very weak (in the low millimolar range). However, the RNA/RNA duplex chosen for the study consisted of (*i*) a 20-mer RNA primer, which contained the 18 nucleotides complementary to the primer binding site (PBS) sequence as well as two nonpairing bases at the 5′ end to avoid problems with blunt-end additions and (*ii*) a 35-mer RNA template containing two 3′-terminal nonpairing bases, the PBS sequence, and a 5′ template overhang of random sequence predicted to have no defined secondary structure. Complex kinetic behavior was observed in both of these studies because of significant nonproductive primer-template binding. This nonproductive primer-template binding mode and complex kinetics may be physiologically relevant. On the other hand, these observations may be related, in part, to primer-template design or the absence of the single-stranded RNA-binding HIV nucleocapsid protein.

To carefully compare the binding and incorporation of the incoming dNTP as well as the release of the elongated primer-template product (P_{n+1}/T) for RT-bound RNA/RNA,

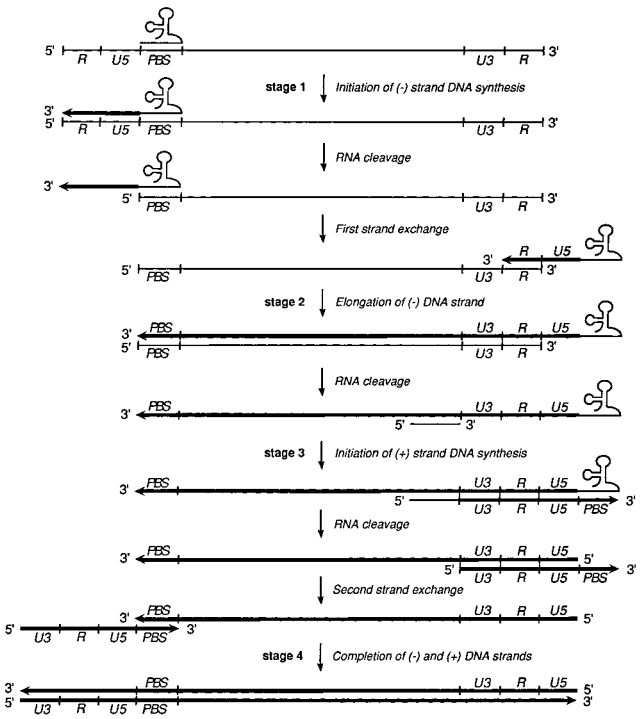

FIGURE 1: Conversion of the single-stranded HIV RNA genome to a double-stranded DNA copy by HIV-1 RT. Reverse transcription involves four stages of DNA synthesis (indicated numerically), cleavage of RNA that is annealed to DNA (RNase H activity), and two strand-switching events. RNA and DNA are represented as thin and thick lines, respectively. The human lysyl tRNA is shown initially annealed to the primer binding site (PBS) of the HIV RNA genome. The relative locations of the U5, U3, and R sequences are also indicated.

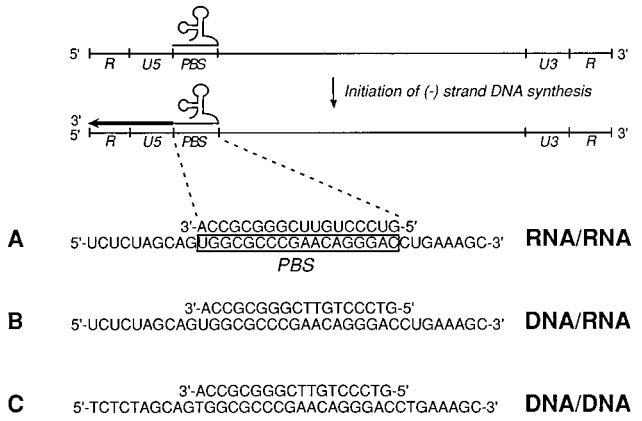

FIGURE 2: The primer-template substrates used in this study. HIV-1 RT initiates in vivo DNA synthesis from a primer-template complex in which the 18 nucleotides at the 3′ end of a human lysyl tRNA primer are annealed to the primer binding site (PBS) of the HIV genomic RNA template. The 18/36-mer RNA/RNA primer-template substrate (A) used in this study consists of (*i*) an 18-nucleotide RNA primer whose sequence is identical to the 3′ end of the human lysyl tRNA and (*ii*) a 36-nucleotide RNA template whose sequence is identical to the HIV genome and which contains the PBS sequence (boxed). The 18/36-mer DNA/RNA (B) and DNA/DNA (C) substrates used are also shown.

DNA/RNA, and DNA/DNA substrates, we designed the primer-template substrates shown in Figure 2, A−C. The RNA and DNA primers were made to be of the same length to avoid the possibility of effects of primer length on primer-template binding that have been observed previously (*22*). Furthermore, to eliminate contributions from the non-PBS-

binding regions of the $tRNA^{Lys}$ (*23*), a short RNA primer was chosen whose sequence is identical to the 18 nucleotides at the 3′-end of the $tRNA^{Lys}$ that bind to the PBS. In addition, the 36-mer RNA template used in this study is identical in sequence to the HIV RNA genome. Although terminal nonpairing bases have been used in blunt-ended primer-template duplexes to avoid blunt-end additions (*21*), we chose a primer-template substrate containing both 5′ and 3′ template overhangs. This primer-template design avoids the possibility of kinetic complexities introduced by RT-catalyzed blunt-end additions that have been observed by our group (*24*) and others (*21*, *25*). Moreover, while blunt-ended primer-template substrates have proven very useful in studying RT, they are, in fact, nonphysiological structures that are not encountered by RT in vivo (see Figure 1).

Using the primer-template substrates shown in Figure 2, A−C, the present study was designed to examine (*i*) the affinity of the incoming dNTP for the RT·primer-template complex (K_d), (*ii*) the rate of dNTP incorporation into the primer (k_{pol}), (*iii*) and the rate of release of the extended-primer-template product (P_{n+1}/T) from RT (k_{ss}). The results from this study provide a quantitative description of the interactions involving RT, the various primer-template substrates, and the incoming dNTP. A model summarizing these results is presented, and implications for the molecular mechanism of initiation of (−) strand DNA synthesis by RT are discussed.

EXPERIMENTAL PROCEDURES

Materials. All chemicals were of analytical or reagent grade and were used without further purification. All water was prepared on a Milli-Q UF Plus Water System including a QPAK_2 purification pack (Millipore). BA85 nitrocellulose membranes (0.45 μM, 4 × 5.25 in) and NA45 DEAE cellulose membranes (0.45 μM, 4 × 5.25 in) were purchased from Schleicher and Shuell. The dCTP was purchased from Pharmacia Biotech. [γ-^{32}P]ATP was obtained from Amersham. The 18-mer RNA primer and the 36-mer RNA template were synthesized by New England BioLabs. The 18-mer DNA primer and the 36-mer DNA template were synthesized by the Keck Oligonucleotide Synthesis Facility at Yale. HIV-1 RT was purified as previously described (*11*, *26*).

General Methods. The concentrations of the RNA and DNA oligomers were determined spectrophotometrically at 260 nm using the calculated extinction coefficients ϵ_{260} = 177 000 $M^{-1}cm^{-1}$ and ϵ_{260} = 396 000 $M^{-1}cm^{-1}$ for the 18-mer and 36-mer RNA oligomers, respectively, and ϵ_{260} = 170 000 $M^{-1}cm^{-1}$ and ϵ_{260} = 388 000 $M^{-1}cm^{-1}$ for the 18-mer and 36-mer DNA oligomers, respectively. The RNAs and DNAs were 5′-labeled with T4 polynucleotide kinase (New England BioLabs) and [γ-^{32}P]ATP. All 18/36-mer duplexes were annealed by incubating a 1:1.4 molar ratio of 18-mer primer (68 Ci $mmol^{-1}$) to 36-mer template (48 Ci $mmol^{-1}$) in 50 mM Tris chloride (pH 7.8) buffer containing 50 mM NaCl at 90 °C for 3 min and 50 °C for 10 min.

The protein concentration of purified RT was measured spectrophotometrically at 280 nm using an extinction coefficient ϵ_{280} = 260 450 $M^{-1}cm^{-1}$. The concentration of active RT was determined as previously described with pre-steady-state burst experiments (*11*) that gave burst amplitudes of 40%, and all enzyme concentrations reported in this study have been corrected using this fraction of active enzyme.

Filter-binding experiments with HIV-1 RT and the 18/36-mer RNA homoduplex were performed as previously described using a nitrocellulose-DEAE membrane double-filter-binding assay with a 96-well double filter dot blot apparatus that had been constructed from a modified acrylic Minifold I dot-blot apparatus from Schleicher and Schuell (*27*, *28*). The nitrocellulose and DEAE membrane filters were prepared as described (*27*). In this assay, HIV-1 RT (10 nM) was preincubated with increasing concentrations (15−1000 nM) of the doubly 5′-[^{32}P]-labeled 18/36-mer RNA homoduplex in buffer [50 mM Tris chloride (pH 7.8), 50 mM NaCl] for ≥1 min at 37 °C. With a vacuum applied to the double-filter dot-blot apparatus, a well was washed with 100 μL of buffer immediately before filtering the sample. After filtering 100 μL of the sample, the well was washed with 100 μL of buffer. This procedure was repeated in triplicate for each concentration of the 18/36-mer RNA homoduplex. The concentration of RT-bound 18/36-mer RNA homoduplex was then determined by phosphorimaging analysis of the nitrocellulose and DEAE membrane filters on a BioRad GS-525 Molecular Imager System. Nonspecific binding of the 18/36-mer RNA homoduplex to the nitrocellulose membrane at each concentration was determined to be negligible (≤0.3%). The observed amplitude in Figure 3 (5.3 nM) is 53% of the expected value of 10 nM based on the active site concentration of HIV-1 RT used in the binding assay. However, the amplitude has been observed to vary, in part, with the strength of the applied vacuum without variations in the value of K_d (Z. Suo and K. A. Johnson, personal communication). Furthermore, similar amplitudes to the one reported here previously have been observed with the binding of duplexes to HIV-1 RT (*28*).

Rapid chemical quench experiments were performed as previously described with a KinTek Instruments Model RQF-3 rapid-quench-flow apparatus thermostated at 37 °C (*11*, *26*). All reactants (RT, primer-template, dCTP, and $MgCl_2$) are reported in their final concentrations after mixing the contents of the two 15-μL sample loops. HIV-1 RT (250 nM) and the doubly 5′-[^{32}P]-labeled 18/36-mer duplex (50 nM) were preincubated on ice for 5 min in buffer [50 mM Tris chloride (pH 7.8), 50 mM NaCl]. Polymerization was initiated at 37 °C by the rapid addition of dCTP (1−2000 μM) in buffer containing 10 mM $MgCl_2$, and the reactions were quenched at the indicated times with 0.3 M EDTA. Products were analyzed on a 20% polyacrylamide gel containing 7.5 M urea and 12% formamide followed by phosphorimaging analysis on a BioRad GS-525 Molecular Imager System.

Data Analyses. The data were fit by nonlinear regression using the program SigmaPlot version 4.14 (Jandel Scientific). The data from the filter binding experiment in Figure 3 was fit to the quadratic equation: $[RT{\cdot}RNA/RNA] = 0.5(K_d+E+[RNA/RNA]) - 0.5\{(K_d+E+[RNA/RNA])^2 - 4E[RNA/RNA]\}^{1/2}$, where K_d is the equilibrium dissociation constant for the RNA/RNA homoduplex and E is the concentration of active sites of HIV-1 RT. The data from the pre-steady-state burst experiment in Figure 4 was fit to a burst equation: $[19\text{-mer}] = A(1 - e^{-k_{obsd}t}) + rt$, where A is the amplitude, k_{obsd} is the observed first-order rate constant

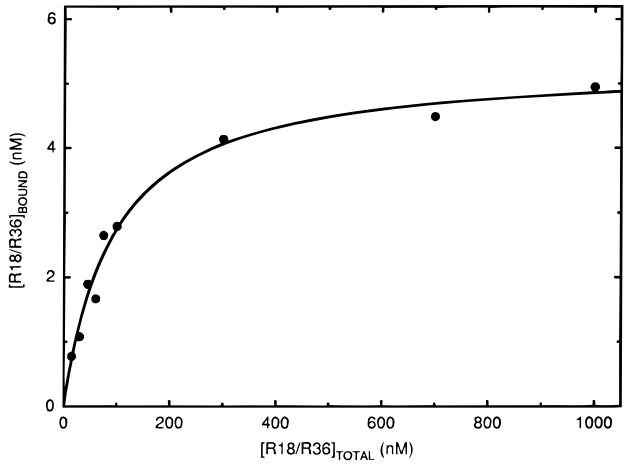

FIGURE 3: Binding of the 18/36-mer RNA duplex to HIV-1 RT. The binding of the 18/36-mer RNA duplex (15−1000 nM) to HIV-1 RT (10 nM) was determined in buffer [50 mM Tris chloride (pH 7.8), 50 mM NaCl] at 37 °C using a double-filter binding assay. The binding of 18/36-mer RNA duplex to HIV-1 RT was fit to a quadratic equation as described, and the curve is drawn for an amplitude $A = 5.3 \pm 0.2$ nM and an equilibrium dissociation constant $K_d = 90 \pm 11$ nM.

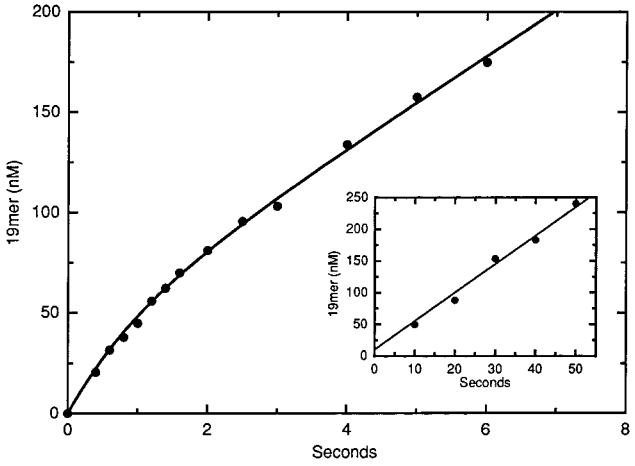

FIGURE 4: Pre-steady-state kinetics of dCMP incorporation by HIV-1 RT. The incorporation of dCMP (2 mM dCTP) into the 18/36-mer RNA duplex (500 nM) by HIV-1 RT (50 nM) was determined at 37 °C in buffer containing 10 mM $MgCl_2$. The time course for dCMP incorporation by HIV-1 RT was fit to a burst equation as described, and the curve is drawn for an amplitude $A = 40 \pm 8$ nM, an observed first-order rate constant $k_{obsd} = 1.0 \pm 0.1$ s^{-1}, and a steady-state rate $r = 23 \pm 2$ nM s^{-1}. The steady-state rate constant k_{ss} ($= r/A$) was calculated to be 0.58 ± 0.13 s^{-1}. *Inset*: Steady-state kinetics of dCMP incorporation by HIV-1 RT. The incorporation of dCMP (2 mM dCTP) into the 18/36-mer RNA duplex (1000 nM) by HIV-1 RT (10 nM) was determined at 37 °C in buffer containing 10 mM $MgCl_2$. From the slope of the line, it was determined that $k_{ss} = 0.45 \pm 0.04$ s^{-1}.

for dCTP incorporation in the burst phase, and r is the linear steady-state rate of product release. The steady-state rate constant k_{ss} was calculated by dividing r by A. The data from the single-turnover experiments (see, for example, Figure 5A) were fit to a single-exponential equation: [19-mer] $= A(1 - e^{-k_{obsd}t})$. The binding curve shown in Figure 5B was fit to the following hyperbolic equation: $k_{obsd} = k_{pol}[dCTP]/(K_d + [dCTP])$, where k_{pol} is the maximum first-order rate constant for dCTP incorporation and K_d is the equilibrium dissociation constant.

RESULTS

The RNA/RNA primer-template substrate shown in Figure 2A was designed to be a physiologically relevant model substrate with which to begin an initial study of the initiation of (−) strand DNA synthesis by HIV-1 RT. Recently, we have used this RNA/RNA substrate to establish that there is a 2.6-fold increase in the selection for incorporation of the natural nucleotide dTTP over the unnatural nucleoside analogue AZTTP by AZT-resistant HIV-1 RT as compared to its wild-type form (*29*).

Binding of RNA/RNA Primer-Template. To estimate the affinity of the 18/36-mer RNA/RNA duplex for HIV-1 RT, a double-filter binding assay was performed. The advantage of this technique is that both RT-bound *and* free 18/36-mer RNA/RNA duplex can be measured. This assay has been used successfully in the past to examine the binding of heteroduplexes to HIV-1 RT (*28*). Figure 3 shows a hyperbolic dependence of the amount of RT-bound 18/36-mer RNA/RNA on the total concentration of 18/36-mer RNA/RNA with an equilibrium dissociation constant (K_d) of 90 nM under conditions in which the concentration of HIV-1 RT is 10 nM (active sites).[2] The amount of RT-bound RNA/RNA duplex was determined in triplicate for each concentration of RNA/RNA, and the standard deviations in the average values were typically ≤13%.

Pre-Steady-State and Steady-State Incorporation of dCTP into RNA/RNA. Based on the sequence of the 36-mer RNA template, the first dNTP to be incorporated into the 18-mer RNA primer is dCTP, which results in the formation of a 19-mer. During reverse transcription in vivo, dCTP is also the first dNTP incorporated into the human $tRNA^{Lys}$ primer by RT though it is unclear whether this event occurs immediately following host cell infection or during the assembly of new virion particles (*23*). As shown in Figure 4, the incorporation of dCTP into the 18/36-mer RNA duplex exhibits burst kinetics under pre-steady-state burst conditions in which the concentration of the 18/36-mer RNA substrate (500 nM) was in a 10-fold excess over the concentration of HIV-1 RT (50 nM). Formation of the 19-mer involves an initial burst phase with an observed first-order rate constant (k_{obsd}) of 1.0 s^{-1}. The magnitude of the burst (40 ± 8 nM) is consistent with the concentration of HIV-1 RT active sites (50 ± 5 nM) used in the experiment. Following the burst is a slower linear steady-state phase with a steady-state rate constant $k_{ss} = 0.58$ s^{-1} that corresponds to the release of the 19/36-mer product from the enzyme. The inset of Figure 4 shows the incorporation of dCTP into the 18/36-mer RNA duplex under steady-state conditions in which the concentration of the 18/36-mer RNA substrate (1000 nM) was in a 100-fold excess over the concentration of HIV-1 RT (10 nM). Under these conditions, the steady-state rate constant (k_{ss}) for 19/36-mer release is 0.45 s^{-1}. This rate constant is

[2] The K_d value of 90 nM determined for the 18/36-mer RNA/RNA duplex using the double-filter binding assay is a measure of both productive and nonproductive binding modes. We are unable to confirm this value using the method of active site titration to measure exclusively the productive binding mode because of the error associated with pre-steady-state burst amplitudes when the burst rate constant is slow as seen in Figure 4. However, it has been shown both empirically and mathematically that the observed affinities determined by either filter binding or active site titration methods should be the same (*28*).

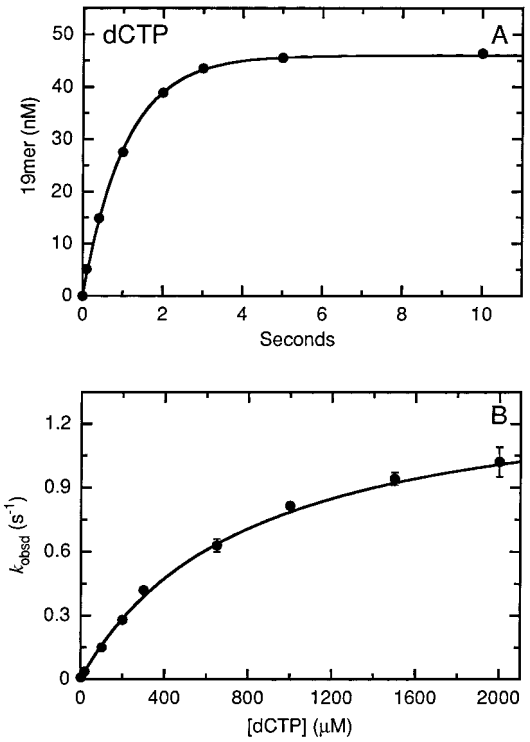

FIGURE 5: Single-turnover dCMP incorporation kinetics and dCTP concentration dependency for HIV-1 RT. (A) The incorporation of dCMP (1.5 mM dCTP) into the 18/36-mer RNA duplex (50 nM) by HIV-1 RT (250 nM) was determined at 37 °C in buffer containing 10 mM $MgCl_2$. The time course for dCMP incorporation by HIV-1 RT was fit to a single-exponential equation as described, and the curve is drawn for an amplitude $A = 46 \pm 1$ nM and an observed first-order rate constant $k_{obsd} = 0.94 \pm 0.03$ s^{-1}. (B) The dependence of k_{obsd} for incorporation of dCMP into the 18/36-mer RNA duplex (50 nM) by HIV-1 RT (250 nM) on the concentration of dCTP (1−2000 μM) was determined at 37 °C in buffer containing 10 mM $MgCl_2$. The dCTP concentration dependence of k_{obsd} for HIV-1 RT was fit to a hyperbolic equation as described, and the curve shown represents a fit for an equilibrium dissociation constant $K_d = 780 \pm 50$ μM and a maximum first-order rate constant for incorporation $k_{pol} = 1.4 \pm 0.1$ s^{-1}

consistent with and confirms the steady-state rate constant determined under pre-steady-state burst conditions.

Single-Turnover Incorporation of dCTP into RNA/RNA. To examine further the kinetics of dCTP incorporation in the burst phase, single-turnover experiments were performed. Figure 5A shows that the incorporation of dCTP to form the 19/36-mer exhibits simple first-order kinetics under the conditions in which the concentration of HIV-1 RT (250 nM) was in a 5-fold excess over the concentration of the 18/36-mer RNA substrate (50 nM). At a concentration of 1.5 mM dCTP, the formation of the 19/36-mer occurred with an observed first-order rate constant $k_{obsd} = 0.94$ s^{-1}. The value of k_{obsd} is independent of the concentration of HIV-1 RT in the range 250−500 nM, which provides evidence that binding of dCTP to the RT·18/36-mer RNA complex or release of the 19/36-mer extended product is not rate limiting. Thus, under these conditions only a single enzyme turnover is being examined. To establish the equilibrium dissociation constant (K_d) for dCTP and the maximum rate constant for polymerization (k_{pol}), the dependence of k_{obsd} on the concentration of dCTP was examined. As shown in Figure 5B, the value of k_{obsd} displays a hyperbolic dependence on the dCTP concentration with $K_d = 780$ μM and $k_{pol} = 1.4$ s^{-1}.

Table 1: Kinetic and Equilibrium Constants for Binding and Incorporation of dCTP by HIV-1 RT

primer/ template	k_{pol} (s^{-1})	K_d (μM)	k_{pol}/K_d (μM^{-1} s^{-1})[a]	k_{ss} (s^{-1})
RNA/RNA	1.4 ± 0.1	780 ± 50	$(1.8 \pm 0.2) \times 10^{-3}$	0.58 ± 0.13
DNA/RNA	46 ± 2	14 ± 2	3.3 ± 0.5	0.11 ± 0.05
DNA/DNA	17 ± 1	11 ± 4	1.5 ± 0.6	0.11 ± 0.02

[a] Error in the value of k_{pol}/K_d was calculated using standard methods (*46*).

Errors in the values of k_{obsd} were typically ≤11%. At all concentrations of dCTP, the amount of product formed upon reaction completion was equal to the initial amount of RNA/RNA primer-template substrate. The value of k_{pol} determined under single-turnover conditions is consistent with and confirms the value of the rate constant obtained from the burst phase of the pre-steady-state burst experiment shown in Figure 4.

Single-Turnover Incorporation of dCTP into DNA/RNA and DNA/DNA Substrates. To directly compare the kinetics of dCTP binding and incorporation for the RNA homoduplex primer-template substrate to that of the corresponding heteroduplex and DNA homoduplex forms, the DNA/RNA (Figure 2B) and DNA/DNA (Figure 2C) versions of the RNA/RNA primer-template substrate shown in Figure 2A were also prepared. Using either the 18/36-mer DNA/RNA or 18/36-mer DNA/DNA primer-template substrates, the dCTP concentration dependence of k_{obsd} was examined under single-turnover conditions as described above. Errors in the values of k_{obsd} were typically ≤14%. The results from these experiments are summarized in Table 1. The rate of dCTP incorporation (k_{pol}) for an RNA/RNA substrate is approximately 33- and 12-fold slower than the values for DNA/RNA and DNA/DNA primer-template substrates, respectively, while the affinity of dCTP (K_d) for the RT·RNA/RNA complex is 56- and 71-fold weaker than the affinities for RT·DNA/RNA and RT·DNA/DNA complexes, respectively. Based on the values for k_{pol} and K_d, the efficiency of incorporation of dCTP (k_{pol}/K_d) into an RNA/RNA substrate is approximately 1800- and 800-fold less than those for DNA/RNA and DNA/DNA substrates, respectively. Table 1 also reports the values of k_{ss} obtained from pre-steady-state burst experiments which show that the steady-state rate of release of the 19/36-mer from the enzyme is about 5-fold faster for an RNA/RNA substrate as compared to either DNA/RNA or DNA/DNA substrates. During the course of performing these single-turnover studies, we did not observe bi- or triphasic kinetic behavior as has been reported for dNTP incorporation into alternate primer-template substrates, which provided evidence for significant nonproductive binding of those duplexes to HIV-1 RT (*20*, *21*). Our observation of simple first-order kinetics for the incorporation of dCTP into the primer-template substrates used in this study as well as the conversion of all of the primer-template substrate (P_n/T) to the elongated primer-template product (P_{n+1}/T) suggests that the great majority of these duplexes are bound productively to HIV-1 RT.

DISCUSSION

Previous mechanistic studies of DNA polymerization by HIV-1 RT have focused primarily on DNA/RNA and DNA/

DNA primer-template (P/T) substrates (*11*−*16*). These studies have shown that both substrates bind tightly and with similar affinities to HIV-1 RT ($K_d \approx 5$ nM). Following formation of the RT·P/T complex, the dNTP then binds in a two-step binding process. The initial step in dNTP binding involves the formation of a transient RT·P/T·dNTP complex in which the incoming dNTP base pairs with the corresponding nucleotide in the template. The formation of this initial ternary complex induces a rate-determining conformational change that limits the rate of chemical catalysis for dNTP incorporation. Single-turnover experiments typically allow the direct observation of the chemistry step in any enzymatic reaction. However, in this case single-turnover studies of HIV-1 RT result in the direct measurement of the relatively slower conformational change that immediately precedes dNTP incorporation. The recently determined structure of an RT·P/T·dNTP ternary complex (*17*), together with previous RT structures (*30*−*32*), demonstrates that this conformational change involves the transition of the enzyme from an inactive open state to an active closed state in which the active site residues become optimally aligned with respect to the bound dNTP so that chemistry may proceed. The rate for formation of this conformation (k_{pol}) was shown to be about 2-fold faster for a DNA/RNA substrate as compared to a DNA/DNA substrate (*11*). The rate of formation of this critical conformation also depends on proper Watson−Crick base pairing between the incoming dNTP and the template (*18*). Previous work from this laboratory has demonstrated that this conformational change plays an important role in DNA replication fidelity since mispairing between an incorrect dNTP and the template does not support the proper alignment of active site residues (*11*, *13*). The slowest step in the overall reaction pathway of HIV-1 RT is the release of the elongated primer-template (P_{n+1}/T) from the enzyme during a single deoxynucleotide incorporation.

While most of these earlier studies focused on DNA/RNA and DNA/DNA substrates of random sequence, the goal of the present study was to understand the mechanism by which HIV-1 RT initiates (−) strand DNA synthesis from a physiologically relevant RNA/RNA primer-template substrate. This event is the first step in the overall pathway catalyzed by HIV-1 RT in which the single-stranded viral RNA genome is converted to a double-stranded DNA copy (Figure 1). *In vivo*, the human $tRNA^{Lys}$ is used by HIV-1 RT as a primer for initiating (−) strand DNA synthesis—the 18 nucleotides at the 3′ end of the $tRNA^{Lys}$ anneal to the primer binding site (PBS) sequence of the 10 kb HIV genomic RNA template. As a first approach to understanding the initiation of (−) strand DNA synthesis, we chose an 18/36-mer RNA/RNA primer-template complex as a model substrate for our studies in which the RNA template is identical to the HIV-1 RNA genomic sequence and the primer is complementary to the PBS (Figure 2A). The overall results of the present study using this RNA/RNA substrate are summarized in Scheme 1. We determined that this RNA duplex binds with reasonably high affinity ($K_d = 90$ nM) to HIV-1 RT (Figure 3); however, it appears that the enzyme has a higher affinity for DNA/RNA and DNA/DNA duplexes ($K_d \approx 5$ nM) (*11*). This observation suggests that RNA/RNA substrates are bound somewhat differently to the enzyme than DNA/RNA or DNA/DNA substrates. Further evidence for a significantly different conformation of the RT·RNA/RNA complex was provided by an examination of the kinetics of dCTP binding and incorporation.

Scheme 1

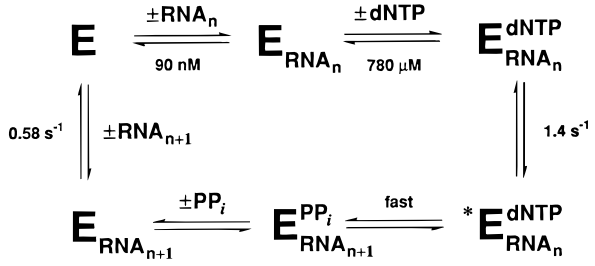

Pre-Steady-State Kinetic Mechanism. The first indication that the kinetics of DNA polymerization by HIV-1 RT were significantly different for an RNA/RNA substrate as compared to DNA/RNA and DNA/DNA substrates can be seen in the pre-steady-state burst experiment shown in Figure 4. In this type of experiment, the primer-template substrate is in excess over the enzyme such that the first enzyme turnover as well as multiple turnovers can be examined simultaneously. We observed a slow, shallow pre-steady-state burst of product formation (1.0 s^{-1}) followed by a slightly slower linear steady-state phase (0.58 s^{-1}). The rate of product formation in the burst phase reflects the rate of dCTP incorporation during the first enzyme turnover. Subsequent turnovers, however, are limited by the relatively slower rate of product release that is manifested as the linear steady-state phase of product formation. The general observation of a burst followed by a linear steady-state phase of product formation for an RNA/RNA substrate is consistent with our previous studies of HIV-1 RT using DNA/RNA and DNA/DNA substrates (*11*, *13*, *33*). However, the rate of dCTP incorporation into an RNA/RNA substrate at this concentration of dCTP was much slower, while the rate of extended-RNA/RNA (19/36-mer) product release was faster. This faster rate of product release was confirmed by performing a steady-state kinetic experiment (Figure 4, inset). Therefore, when compared to the corresponding DNA/RNA (Figure 2B) and DNA/DNA (Figure 2C) versions of the RNA/RNA substrate shown in Figure 2A, the release of the extended-RNA primer/RNA template product from HIV-1 RT is approximately 5-fold faster than the release of extended-DNA/RNA and extended-DNA/DNA products, respectively (see Table 1). The observation of a faster release rate is also consistent with our finding of a decrease in the affinity of HIV-1 RT for the RNA duplex.

Following this confirmation of a faster rate of release for the extended-RNA/RNA product, we focused our attention on the slow pre-steady-state burst of product formation. To confirm that this rate was indeed relatively slow, the rate of dCMP incorporation into the RNA/RNA substrate at the active site of HIV-1 RT was measured under single-turnover conditions. As shown by the time course in Figure 5A, the incorporation of dCMP occurred with an observed first-order rate constant k_{obsd} of 0.94 s^{-1}. This slower-than-expected rate suggested that one or both of the following had occurred: (*i*) the affinity of dCTP for the HIV-1 RT·RNA/RNA complex had decreased and (*ii*) the maximum rate of dCMP incorporation had decreased. For this reason the equilibrium dissociation constant (K_d) and maximum rate of polymerization (k_{pol}) values for dCTP were then determined by

examining the dependence of k_{obsd} for dCTP incorporation on the concentration of dCTP (Figure 5B). The affinity of dCTP (780 μM) for the HIV-1 RT·RNA/RNA complex was found to be relatively weaker compared to the affinities for the corresponding RT·DNA/RNA and RT·DNA/DNA complexes (see Table 1), which is consistent with earlier studies of dTTP binding (*21*). The rate of dCTP incorporation into the RNA/RNA primer-template substrate (1.4 s^{-1}) was found to be slower as compared to the corresponding DNA/RNA and DNA/DNA substrates (see Table 1). The slow rate observed in the current study is consistent with an earlier report using a modified bovine $tRNA^{Lys}$ primer (*20*). These similar rates suggest that the slow rate of dNTP incorporation is the result of the conformation of the RT·RNA/RNA complex and not the presence of a bulky $tRNA^{Lys}$ or its interactions with non-PBS template sequences. In addition, the weaker affinity and slower rate of incorporation for dCTP when using an RNA/RNA substrate may not be restricted to HIV-1 RT. Rather, it may be a general feature of DNA polymerases that must attach a deoxynucleotide to an RNA primer (for example, during lagging strand DNA synthesis).

Structural Consequences of RNA-Primed DNA Polymerization. The observation of a weaker affinity of dCTP for the HIV-1 RT·RNA/RNA complex provides evidence that suggests that the nucleotide binding pocket of the HIV-1 RT·RNA/RNA complex exists in a significantly different conformation as compared to those of the corresponding HIV-1 RT·DNA/RNA and HIV-1 RT·DNA/DNA complexes. In addition, the slower rate of dCTP incorporation at the active site of the HIV-1 RT·RNA/RNA complex suggests that it is more difficult to achieve a conformation that includes optimal alignment of the active site residues as well as proper Watson−Crick base pairing between the incoming dNTP and the template.[3] During the initiation of (−) strand DNA synthesis from an RNA/RNA primer-template duplex, HIV-1 RT is required to be sufficiently flexible to accommodate the structural transition from an A-form RNA duplex to a non-A, non-B H-form DNA/RNA hybrid. Moreover, at the beginning of this transition, a chimeric RNA−DNA junction is formed upon dCTP incorporation into the RNA primer, which remains annealed to the RNA template. While an A-form RNA duplex has a very wide minor groove and consists of sugars in the C3′-endo conformation (*36*), an H-form DNA/RNA heteroduplex has a minor groove that is narrower and contains DNA residues with sugars generally in the O4′-endo conformation (*37*). On a molecular level, one can speculate that the structural discontinuities in the chimeric RNA−DNA/RNA duplex may produce a structural feature at or near the RNA−DNA junction which may influence the binding and incorporation of the next incoming dNTP (*29*). Such a feature may include a bend, which has been observed in an RNA−DNA chimera that is annealed to DNA (*38*). However, in the absence of structural information for a chimeric RNA−DNA/RNA duplex, the maximal conclusion that can be made based on the results of this study is that the HIV-1 RT·RNA/RNA complex exists in an alternate conformation which decreases the affinity of the incoming dCTP as well as its rate of incorporation but increases the rate of release of the extended primer-template product as compared to the HIV-1 RT·DNA/RNA and HIV-1 RT·DNA/DNA complexes.

Implications for In Vivo (−) Strand Strong-Stop DNA Synthesis. Although the results of the present study provide evidence for the existence of an alternate conformation of the HIV-1 RT·RNA/RNA·dCTP complex, the physiological significance of this conformation and its kinetic properties during the initiation of (−) strand DNA synthesis in vivo is unclear. It may be useful, however, to consider the following:

(1) *Initiation of (−) Strand DNA Synthesis is a Rate-Limiting Step in HIV-1 Replication.* Compared to dNTP incorporation into DNA/RNA and DNA/DNA duplexes, the incorporation of dCTP by HIV-1 RT into the RNA/RNA primer-template substrate is the slowest. Overall, this slow rate, together with the decreased affinity of dCTP, results in an approximate 1000-fold reduction in the efficiency of incorporation relative to that of the DNA/RNA and DNA/DNA substrates. In addition to being a measure of incorporation efficiency, k_{pol}/K_d also provides a lower limit on the value of the second-order rate constant for the binding of dCTP to the HIV-1 RT·RNA/RNA complex. Therefore, the large decrease in the value of k_{pol}/K_d implies that the rate of dCTP binding to the HIV-1 RT·RNA/RNA complex is much slower than the rates for dCTP binding to the HIV-1 RT·DNA/RNA and HIV-1 RT·DNA/DNA complexes. A slower rate of dCTP binding would suggest that following a collision between dCTP and HIV-1 RT·RNA/RNA, it is more difficult for the molecule of dCTP to orient itself in such a way that leads to productive binding. Stopped-flow fluorescence measurements will be required to determine directly if the second-order rate constant for dCTP binding has indeed decreased.

(2) *The Current Study was performed with a Model RNA/RNA Substrate.* It is possible that the full-length natural $tRNA^{Lys}$ is required for the formation and stabilization of an HIV-1 RT·$tRNA^{Lys}$/RNA·dCTP complex, whose conformation is better poised for initiation. Other intermolecular interactions may also be required to reestablish the structural features of the true $tRNA^{Lys}$/HIV genome RNA/RNA duplex. For example, chemical and enzymatic probing studies performed in the absence of RT have shown that the anticodon loop of the $tRNA^{Lys}$ interacts with an A-rich loop of a hairpin structure upstream of the PBS (*39*, *40*). Deletion of this A-rich loop from the RNA genomic template results in a reduction in viral replication in vivo and decreased (−) strand DNA synthesis in vitro, thus providing evidence for

[3] The use of α-thio-dCTP in a single-turnover experiment resulted in approximately a 10-fold decrease, relative to dCTP, in the rate of incorporation. However, this thio effect is difficult to interpret since we cannot exclude the possibility that the presence of the bulkier sulfur atom may reduce the rate of optimal positioning of active site residues, Mg^{2+}, and RNA/RNA primer-template during the conformational change (*34*). Therefore, we cannot exclude the possibility of a slow rate of chemical catalysis (attachment of dCTP to the 3′-end of the RNA primer) that is no longer limited by the preceding conformational change. However, this possibility seems unlikely for the following two reasons. First, the rate of dNTP attachment to the 3′-OH of a DNA primer has been estimated to be ≥9000 s^{-1} (*35*). If the rate that we observe for dCMP incorporation into the 18-mer RNA primer (1.4 s^{-1}) were a measure of chemical catalysis rather than the conformational change that precedes chemistry, then the incorporation of a dNTP into an RNA primer would be ≥ 9000-fold less favorable than incorporation into a DNA primer. It seems thermodynamically unlikely that the rate of chemistry would decrease by ≥ 10^4 for an RNA primer. Second, we have also measured the rate of incorporation of the next correct dNTP following dCTP which is dTTP (*29*). This dTTP incorporation rate is also relatively slow (0.76 s^{-1}) even though now the chemistry involves attaching a deoxynucleotide to another deoxynucleotide rather than attaching a deoxynucleotide to a ribonucleotide.

the importance of the A-rich loop in HIV-1 reverse transcription (*41*). In addition, template−template interactions have been identified between the two copies of the HIV RNA genome near their 5′-ends (*42*). Although these intermolecular interactions may be important at some stage of reverse transcription, a study of the initiation of (−) strand DNA synthesis using a substrate consisting of a natural $tRNA^{Lys}$ primer annealed to a longer genomic RNA template (>300 nucleotides) showed that the rate of dNTP incorporation is just as slow (0.2 s^{-1}) (*20*) as the rates reported here and elsewhere (*21*, *29*). This observation argues against the notion that the $tRNA^{Lys}$ and its interactions with the genomic RNA template are the minimal requirements for a more catalytically active initiation complex.

(3) *Other Factors may be required to Activate Catalysis in the Initiation Complex.* The formation, stability, and catalytic activity of the HIV-1 RT·RNA/RNA·dCTP complex may be augmented in vivo by the presence of cellular or other viral factors that are involved in viral replication. One potential factor is the HIV nucleocapsid protein (*43*), a small basic Zn^{2+} finger-containing protein that binds to single-stranded regions of RNA (*44*) and interacts with HIV-1 RT (*45*). Other factors may include precursors of the *gag-pol* genes of HIV as well as β-actin (*23*).

Conclusions. We propose that the active site of the HIV-1 RT·RNA/RNA·dCTP complex exists in a significantly altered conformation as compared to complexes involving DNA/RNA and DNA/DNA substrates. This conclusion is supported by the observations that the affinity of dCTP is weaker, the incorporation of dCTP is slower, and the release of the extended-primer-template product is faster for an RNA/RNA substrate compared to DNA/RNA and DNA/DNA substrates. Overall, the unique kinetic and structural properties of the initiation complex make it an additional therapeutic target for the development of novel inhibitors of HIV-1 replication.

ACKNOWLEDGMENT

We thank Dr. Stephen Hughes, Dr. Paul Boyer, and Dr. Andrea Ferris for the generous gift of the wildtype RT clone, and Dr. Cathy Joyce, Dr. Janice Pata, and Brad King for technical advice and discussions.

REFERENCES

1. De Clercq, E. (1994) *Biochem. Pharmacol. 47*, 155.
2. Goff, S. P. (1990) *J. Acquired Immune Defic. Syndr. 3*, 817.
3. Mitsuya, H., Yarchoan, R., and Broder, S. (1990) *Science 249*, 1533.
4. Richman, D. D., Rosenthal, A. S., Skoog, M., Eckner, R. J., Chou, T.-C., Sabo, J. P., and Merluzzi, V. J. (1991) *Antimicrob. Agents Chemother. 35*, 305.
5. Yarchoan, R., Mitsuya, H., and Broder, S. (1989) *Am. J. Med. 87*, 191.
6. Larder, B. A., Darby, G., and Richman, D. D. (1989) *Science 243*, 1731.
7. Johnson, K. A. (1986) *Methods Enzymol. 134*, 677.
8. Anderson, K. S., and Johnson, K. A. (1990) *Chem. Rev. 90*, 1131.
9. Johnson, K. A. (1992) *Enzymes 20*, 1.
10. Johnson, K. A. (1995) *Methods Enzymol. 249*, 38.
11. Kati, W. M., Johnson, K. A., Jerva, L. F., and Anderson, K. S. (1992) *J. Biol. Chem. 267*, 25988.
12. Spence, R. A., Kati, W. M., Anderson, K. S., and Johnson, K. A. (1995) *Science 267*, 988.
13. Kerr, S. G., and Anderson, K. S. (1997) *Biochemistry 36*, 14056.
14. Hsieh, J. C., Zinnen, S., and Modrich, P. (1993) *J. Biol. Chem. 268*, 24607.
15. Reardon, J. E. (1993) *J. Biol. Chem. 268*, 8743.
16. Rittinger, K., Divita, G., and Goody, R. S. (1995) *Proc. Natl. Acad. Sci. U.S.A. 92*, 8046.
17. Huang, H., Verdine, G. L., Chopra, R., and Harrison, S. C. (1998) *Science 282*, 1669.
18. Johnson, K. A. (1993) *Annu. Rev. Biochem. 62*, 685.
19. Arts, E. J., and Wainberg, M. A. (1996) *Adv. Virus Res. 46*, 97.
20. Lanchy, J.-M., Ehresmann, C., Le Grice, S. F. J., Ehresmann, B., and Marquet, R. (1996) *EMBO J. 15*, 7178.
21. Thrall, S. H., Krebs, R., Wöhrl, B. M., Cellai, L., Goody, R. S., and Restle, T. (1998) *Biochemistry 37*, 13349.
22. Reardon, J. E., Furfine, E. S., and Cheng, N. (1991)*J. Biol. Chem. 266*, 14128.
23. Arts, E. J., and Le Grice, S. F. J. (1998) *Prog. Nucleic Acid Res. Mol. Biol. 58*, 339.
24. Feng, J., and Anderson, K. S. (1999) *Biochemistry 38*, 9440.
25. Patel, P. H., and Preston, B. D. (1994) *Proc. Natl. Acad. Sci. U.S.A. 91*, 549.
26. Kerr, S. G., and Anderson, K. S. (1997) *Biochemistry 36*, 14064.
27. Wong, I., and Lohman, T. M. (1993) *Proc. Natl. Acad. Sci. U.S.A. 90*, 5428.
28. Suo, Z., and Johnson, K. A. (1997) *Biochemistry 36*, 12459.
29. Vaccaro, J. A., and Anderson, K. S. (1998) *Biochemistry 37*, 14189.
30. Kohlstaedt, L. A., Wang, J., Friedman, J. M., Rice, P. A., and Steitz, T. A. (1992) *Science 256*, 1783.
31. Jacobo-Molina, A., Ding, J., Nanni, R., Clark, A. D., Lu, X., Tantillo, C., Williams, R. L., Kamer, G., Ferris, A. L., Clark, P., Hizi, A., Hughes, S. H., and Arnold, E. (1993) *Proc. Natl. Acad. Sci. U.S.A. 90*, 6320.
32. Rodgers, D. W., Gamblin, S. J., Harris, B. A., Ray, S., Culp, J. S., Hellmig, B., Woolf, D. J., Debouck, C., and Harrison, S. C. (1995) *Proc. Natl. Acad. Sci. U.S.A. 92*, 1222.
33. Feng, J. Y., and Anderson, K. S. (1999) *Biochemistry 38*, 55.
34. Admiraal, S. J., Schneider, B., Meyer, P., Janin, J., Véron, M., Deville-Bonne, D., and Herschlag, D. (1999) *Biochemistry 38*, 4701.
35. Patel, S. S., Wong, I., and Johnson, K. A. (1991) *Biochemistry 30*, 511.
36. Saenger, W. (1984) in *Principles of Nucleic Acids Structure*, Springer, New York.
37. Salazar, M., Fedoroff, O. Y., Miller, J. M., Ribeiro, N. S., and Reid, B. R. (1993) *Biochemistry 32*, 4207.
38. Fedoroff, O., Salazar, M., and Reid, B. R. (1996) *Biochemistry 35*, 11070.
39. Isel, C., Marquet, R., Keith, G., Ehresmann, C., and Ehresmann, B. (1993) *J. Biol. Chem. 68*, 25269.
40. Isel, C., Ehresmann, C., Keith, G., Ehresmann, B., and Marquet, R. (1995) *J. Mol. Biol. 247*, 236.
41. Liang, C., Li, X., Rong, L., Inouye, P., Quan, Y., Kleiman, L., and Wainberg, M. A. (1997) *J. Virol. 71*, 5750.
42. Paillart, J. C., Marquet, R., Skripkin, E., Ehresmann, C., and Ehresmann, B. (1996) *Biochimie 78*, 639.
43. Mak, J., and Kleiman, L. (1997) *J. Virol. 71*, 8087.
44. You, J. C., and McHenry, C. S. (1993) *J. Biol. Chem. 268*, 16519.
45. Druillennec, S., Caneparo, A., de Rocquigny, H., and Roques, B. P. (1999) *J. Biol. Chem. 274*, 11283.
46. Skoog, D. A., and Leary, J. J. (1992) in *Principles of Instrumental Analysis*, 4th ed., Saunders College Publishing, New York.

BI990945X